

Mixed convection boundary-layer flow from a horizontal circular cylinder with a constant surface heat flux

R. Nazar, N. Amin, I. Pop

Abstract The laminar mixed convection boundary-layer flow of a viscous and incompressible fluid past a horizontal circular cylinder, which is maintained at a constant heat flux and is placed in a stream flowing vertically upward has been theoretically studied in this paper. The solutions for the flow and heat transfer characteristics are evaluated numerically for different values of the mixed convection parameter λ with the Prandtl number $Pr = 1$ and 7, respectively. It is found, as for the case of a heated or cooled cylinder, considered by Merkin [5], that assisting flow delays separation of the boundary-layer and can, if the assisting flow is strong enough, suppress it completely. The opposing flow, on the other side, brings the separation point nearer to the lower stagnation point and for sufficiently strong opposing flows there will not be a boundary-layer on the cylinder.

a radius of the cylinder, m
 C_f local skin friction coefficient
 g acceleration due to gravity, m/s^2
 Gr Grashof number
 k thermal conductivity, $W/m\ K$
 Pr Prandtl number
 Re Reynolds number
 q_w heat flux, W/m^2
 T fluid temperature, K
 u, v non-dimensional velocity components along x and y directions, respectively
 $u_e(x)$ non-dimensional velocity outside boundary-layer
 U_∞ free stream velocity, m/s

x, y non-dimensional Cartesian coordinates along the surface of the cylinder and normal to it, respectively
 β thermal expansion coefficient, K^{-1}
 λ mixed convection parameter
 θ non-dimensional temperature
 ν kinematic viscosity, m^2/s
 ψ non-dimensional stream function
' differentiation with respect to y
– dimensional variables
 w condition at the wall
 ∞ ambient condition

1 Introduction

Mixed convection flow past horizontal cylinders is important in situations encountered in the areas of geothermal power generation and drilling operation when the free stream velocity and the induced buoyancy velocity are of comparable order and has received much attention. It continues to be one of the most important problems also due to its fundamental nature as well as many engineering applications. In spite of the fact that a good number of theoretical and experimental studies were carried out in the past on mixed convection flow, it seems that most of these studies are limited to cases in which the forced flow is directed upward (assisting flow).

It appears that the first theoretical study on mixed convection flow from bodies in the existence of a boundary-layer has been carried out by Acrivos [1] who obtained values of the local Nusselt number for the case of a stagnation flow when the Prandtl number $Pr \rightarrow 0$ or $Pr \rightarrow \infty$. Joshi and Sukhatme [2] used a series solution method to study the boundary-layer flow in this problem for both cases of assisting and opposing flow, respectively. Their study was limited to the region from the lower stagnation point up to the point of boundary-layer separation only. Nakai and Okazaki [3] studied the problem of mixed convection from a circular cylinder for the cases when both the Reynolds number Re and Grashof number Gr are very small and also when either forced convection or free convection is dominant. Their results were found to agree reasonably with experimental data for the case of assisting flow but a considerable difference was found in the case of opposing flow. Sparrow and Lee [4] considered the assisting flow regime of this problem and obtained a similarity solution of the boundary-layer equations using an

Received: 28 January 2002
Published online: 6 December 2002
© Springer-Verlag 2002

R. Nazar, N. Amin
Department of Mathematics, Universiti Teknologi Malaysia,
81310 Johor Bahru, Johor, Malaysia

I. Pop (✉)
Faculty of Mathematics, University of Cluj,
R-3400 Cluj, CP 253, Romania
E-mail: popi@math.ubbcluj.ro

The authors wish to thank the Ibn Sina Institute for Fundamental Science Studies of Universiti Teknologi Malaysia for financial support and for giving one of the authors (IP) the chance to visit this University. Part of this paper has been also completed while the senior author (IP) has visited the Brandenburg Technical University of Cottbus, Germany with the support from the Alexander von Humboldt-Stiftung.

approximate expression for the velocity variation outside the boundary-layer. The local Nusselt number distribution was only obtained in the region upstream of the point of boundary-layer separation (from the lower stagnation point up to an angle of 70°). Merkin [5] has studied the same problem by obtaining a numerical solution to the boundary-layer equations based on the assumption that $Re \gg 1$ and $Gr \gg 1$ with $Pr = 1$. The solution was again restricted to the region preceding the point of boundary-layer separation since the boundary-layer equations are not valid beyond that point. Badr [6, 7] studied the mixed convection heat transfer from an isothermal horizontal circular cylinder based on the solution of the full Navier-Stokes and energy equations. Both the cases of assisting and opposing flows were considered. The velocity and thermal boundary layers are developed in time until reaching the steady state conditions. Recently, Aldos et al. [8, 9] investigated the effect of a radial magnetic field on the flow and heat transfer characteristics of mixed convection boundary-layer flow from a horizontal circular cylinder with variable surface temperature. Two sets of transformations were used, one for forced convection-dominated flow and the other for free convection-dominated flow, respectively. The results were obtained numerically using the local nonsimilarity method and the coordinate perturbation method. It should be noted to this end that the unsteady boundary-layer flow from a horizontal circular cylinder has been studied by Katagiri and Pop [10], and Ingham and Merkin [11].

All of the above studies are for a cylinder with constant surface temperature. However, an important practical and experimental circumstance in many convective flows is that generated adjacent to a surface dissipating heat uniformly. The aim of the present paper is therefore, to study the steady mixed convection boundary-layer flow past a horizontal circular cylinder subjected to a constant surface heat flux. The formulation follows closely that proposed by Merkin [5] and the transformed nonsimilar boundary-layer equations are solved numerically using a very efficient technique known as the Keller-box method. The numerical results have been obtained for several values of the mixed convection parameter λ and two values of the Prandtl number Pr , namely, $Pr = 1$ and 7 , respectively. The results refer to the skin friction coefficient, the wall temperature distribution, the position of the boundary-layer separation, as well as to the velocity and temperature profiles near the lower stagnation point. Results were given in the form of tables and graphs, as well. Such tables are very important because they can serve as a reference against which other exact or approximate solutions can be compared in the future.

2 Mathematical formulation

Consider the problem of a horizontal circular cylinder of radius a that is maintained at a constant surface heat flux q_w and is placed in a constant free stream temperature T_∞ . It is assumed that the constant free stream velocity is $(1/2)U_\infty$, so that the velocity outside the boundary-layer is $\bar{u}_e(\bar{x}) = U_\infty \sin(\bar{x}/a)$. It is also assumed that the free stream velocity is directed vertically

upward with $q_w > 0$ for assisting flow and $q_w < 0$ for opposing flow, respectively. The cylinder is considered to be long enough so that the end effects can be neglected and accordingly the flow field can be assumed two-dimensional. Under these assumptions along with the Boussinesq and boundary-layer approximations, the basic equations are:

$$\frac{\partial \bar{u}}{\partial \bar{x}} + \frac{\partial \bar{v}}{\partial \bar{y}} = 0 \quad (1)$$

$$\bar{u} \frac{\partial \bar{u}}{\partial \bar{x}} + \bar{v} \frac{\partial \bar{u}}{\partial \bar{y}} = \bar{u}_e \frac{d\bar{u}_e}{d\bar{x}} + \nu \frac{\partial^2 \bar{u}}{\partial \bar{y}^2} + g\beta(T - T_\infty) \sin\left(\frac{\bar{x}}{a}\right) \quad (2)$$

$$\bar{u} \frac{\partial T}{\partial \bar{x}} + \bar{v} \frac{\partial T}{\partial \bar{y}} = \frac{\nu}{Pr} \frac{\partial^2 T}{\partial \bar{y}^2} \quad (3)$$

subject to the boundary conditions:

$$\bar{u} = \bar{v} = 0, \quad \frac{\partial T}{\partial \bar{y}} = -\frac{q_w}{k} \quad \text{on } \bar{y} = 0 \quad (4a)$$

$$\bar{u} \rightarrow \bar{u}_e(\bar{x}), \quad T \rightarrow T_\infty, \quad \text{as } \bar{y} \rightarrow \infty \quad (4b)$$

where \bar{x} is the coordinate measured along the surface of the cylinder starting from the lower or upper stagnation point, respectively, and \bar{y} is the distance measured normal to it, (\bar{u}, \bar{v}) are the velocity components along the (\bar{x}, \bar{y}) axes, and T , ν , g , β , k and Pr are the local fluid temperature, kinematic viscosity, gravitational acceleration, coefficient of thermal expansion, thermal conductivity and Prandtl number, respectively.

The above equations can be non-dimensionalised using the following new variables:

$$x = \bar{x}/a, \quad y = Re^{1/2}(\bar{y}/a), \quad u = \bar{u}/U_\infty, \quad v = Re^{1/2}(\bar{v}/U_\infty)$$

$$u_e(x) = \bar{u}_e(\bar{x})/U_\infty, \quad \theta = (q_w a/k) Re^{1/2}(T - T_\infty) \quad (5)$$

where $Re = U_\infty a/\nu$ is the Reynolds number. Substituting variables (5) into Eqs. (1)–(3) leads to the following non-dimensional equations:

$$\frac{\partial u}{\partial x} + \frac{\partial v}{\partial y} = 0 \quad (6)$$

$$u \frac{\partial u}{\partial x} + v \frac{\partial u}{\partial y} = u_e \frac{du_e}{dx} + \frac{\partial^2 u}{\partial y^2} + \lambda \theta \sin x \quad (7)$$

$$u \frac{\partial \theta}{\partial x} + v \frac{\partial \theta}{\partial y} = \frac{1}{Pr} \frac{\partial^2 \theta}{\partial y^2} \quad (8)$$

and the boundary conditions (4) become:

$$u = v = 0, \quad \frac{\partial \theta}{\partial y} = -1 \quad \text{on } y = 0 \quad (9a)$$

$$u \rightarrow u_e(x), \quad \theta \rightarrow 0 \quad \text{as } y \rightarrow \infty \quad (9b)$$

where λ is the mixed convection parameter, which can be written as:

$$\lambda = g\beta q_w a^2 \text{Re}^{-1/2} / (kU_\infty^2) = \frac{\text{Gr}}{\text{Re}^{5/2}} \quad (10)$$

in terms of the Grashof number $\text{Gr} = g\beta q_w a^4 / (k\nu^2)$. We notice that $\lambda > 0$ for aiding flow ($q_w > 0$) and $\lambda < 0$ for opposing flow ($q_w < 0$), respectively.

3
Solution procedure

To solve Eqs. (6)–(8), subject to the boundary conditions (9), we assume the following variables:

$$\psi = xF(x, y), \quad \theta = \theta(x, y) \quad (11)$$

where ψ is the stream function defined in the usual way as:

$$u = \frac{\partial\psi}{\partial y}, \quad v = -\frac{\partial\psi}{\partial x} \quad (12)$$

Using (11) and (12) in Eqs. (6)–(8), we get, after some algebra, the resulting equations:

$$\begin{aligned} \frac{\partial^3 F}{\partial y^3} + F \frac{\partial^2 F}{\partial y^2} - \left(\frac{\partial F}{\partial y}\right)^2 + \frac{\sin x \cos x}{x} + \lambda \frac{\sin x}{x} \theta \\ = x \left(\frac{\partial F}{\partial y} \frac{\partial^2 F}{\partial x \partial y} - \frac{\partial F}{\partial x} \frac{\partial^2 F}{\partial y^2} \right) \end{aligned} \quad (13)$$

$$\frac{1}{\text{Pr}} \frac{\partial^2 \theta}{\partial y^2} + F \frac{\partial \theta}{\partial y} = x \left(\frac{\partial F}{\partial y} \frac{\partial \theta}{\partial x} - \frac{\partial F}{\partial x} \frac{\partial \theta}{\partial y} \right) \quad (14)$$

subject to the boundary conditions:

$$F = \frac{\partial F}{\partial y} = 0, \quad \frac{\partial \theta}{\partial y} = -1 \quad \text{on } y = 0 \quad (15a)$$

$$\frac{\partial F}{\partial y} \rightarrow \frac{\sin x}{x}, \quad \theta \rightarrow 0 \quad \text{as } y \rightarrow \infty \quad (15b)$$

It can be seen that near the lower stagnation point of the cylinder, i.e. $x \approx 0$, Eqs. (13) and (14) reduce to the following ordinary differential equations:

$$F''' + FF'' - F'^2 + 1 + \lambda\theta = 0 \quad (16)$$

$$\frac{1}{\text{Pr}} \theta'' + F\theta' = 0 \quad (17)$$

subject to the boundary conditions:

$$F(0) = F'(0) = 0, \quad \theta'(0) = -1 \quad (18a)$$

$$F' \rightarrow 1, \quad \theta \rightarrow 0 \quad \text{as } y \rightarrow \infty \quad (18b)$$

where primes denote differentiation with respect to y .

In practical applications, the physical quantities of principal interest are the local wall temperature and the skin friction coefficient, which are defined, in non-dimensional form, as:

$$\theta(x, 0) = \theta_w(x), \quad C_f = x \left(\frac{\partial^2 F}{\partial y^2} \right)_{y=0} \quad (19a, b)$$

For large values of λ ($\gg 1$), a solution of Eqs. (16) and (17) can be found using the transformation:

$$F(y) = \lambda^{1/5} f(\eta), \quad \theta(y) = \lambda^{-1/5} g(\eta), \quad \eta = \lambda^{1/5} y \quad (20)$$

Substituting (20) into Eqs. (16) and (17) they become:

$$f''' + ff'' - f'^2 + g + \lambda^{-4/5} = 0 \quad (21)$$

$$\frac{1}{\text{Pr}} g'' + fg' = 0 \quad (22)$$

subject to the boundary conditions:

$$f(0) = f'(0) = 0, \quad g'(0) = -1 \quad (23a)$$

$$f' \rightarrow \lambda^{-2/5}, \quad g \rightarrow 0 \quad \text{as } \eta \rightarrow \infty \quad (23b)$$

where primes now denote differentiation with respect to η .

A solution of Eqs. (21) and (22) is sought in the form of series:

$$f = f_0(\eta) + \lambda^{-2/5} f_1(\eta) + \lambda^{-4/5} f_2(\eta) + \dots \quad (24)$$

$$g = g_0(\eta) + \lambda^{-2/5} g_1(\eta) + \lambda^{-4/5} g_2(\eta) + \dots$$

for $\lambda \gg 1$, where the functions $f_0(\eta)$ and $g_0(\eta)$ are given by the equations:

$$f_0''' + f_0 f_0'' - f_0'^2 + \theta_0 = 0 \quad (25)$$

$$\frac{1}{\text{Pr}} \theta_0'' + f_0 \theta_0' = 0 \quad (26)$$

subject to boundary conditions:

$$f_0(0) = f_0'(0) = 0, \quad \theta_0'(0) = -1, \quad (27a)$$

$$f_0' \rightarrow 0, \quad \theta_0 \rightarrow 0 \quad \text{as } \eta \rightarrow \infty \quad (27b)$$

We notice that Eqs. (25)–(27) describe the free convection boundary-layer flow from the lower stagnation point $x \approx 0$ of a horizontal circular cylinder with a constant surface heat flux. The equations for the functions $f_i(\eta)$ and $g_i(\eta)$ ($i \geq 1$) can be written as:

$$f_i''' + \sum_{j=0}^i (f_{i-j} f_j'' - f_{i-j}' f_j') + \theta_i + \delta_{2i} = 0 \quad (28)$$

$$\frac{1}{\text{Pr}} \theta_i'' + \sum_{j=0}^i f_{i-j} \theta_j' = 0 \quad (29)$$

$$f_i(0) = f_i'(0) = 0, \quad \theta_i'(0) = 0 \quad (30a)$$

$$f_i' \rightarrow \delta_{1i}, \quad \theta_i \rightarrow 0 \quad \text{as } \eta \rightarrow \infty \quad (30b)$$

where δ_{1i} and δ_{2i} are the Kronecker delta operators.

On solving Eqs. (25) and (26) for $f_0(\eta)$ and $g_0(\eta)$, and Eqs. (28) and (29) for $f_i(\eta)$ and $g_i(\eta)$ ($i = 1$ and 2), we can express the reduced skin friction $F''(0)$ and the reduced wall temperature distribution $\theta(0)$ valid for large values of λ ($\gg 1$) as:

$$\begin{aligned}
 F''(0) &= \lambda^{3/5} [f_0''(0) + \lambda^{-2/5} f_1''(0) + \lambda^{-4/5} f_2''(0) + \dots] \\
 \theta(0) &= \lambda^{-1/5} [g_0(0) + \lambda^{-2/5} g_1(0) + \lambda^{-4/5} g_2(0) + \dots]
 \end{aligned}
 \tag{31}$$

4 Results and discussion

Equations (13) and (14) subject to the boundary conditions (15) have been solved numerically using a very efficient implicit finite-difference method known as the Keller-box scheme along with the Newton's linearization technique as described by Cebeci and Bradshaw [12]. The numerical solution starts at the lower stagnation point of the cylinder $x \approx 0$ with the initial profiles as given by Eqs. (16) and (17) subject to the boundary conditions (18) and proceed round the cylinder up to the boundary-layer separation point. The actual value of λ which first gives no separation is difficult to determine exactly. It has to be found by successive integrations of the equations. A further difficulty is encountered as the numerical solution indicates that very close to the point $x = \pi$, there is an increase in the skin friction coefficient C_f and a decrease in the surface (wall) temperature distribution $\theta_w(x)$ for solutions with λ near this value (which first gives no separation). For the position of the boundary-layer separation points x_s , decreasing from the upper stagnation point to the lower stagnation point, they are determined, likewise, by successive integrations of the equations, given certain values of λ . The numerical results also show that, in those cases when the boundary-layer separates, $C_f \rightarrow 0$ and $\theta_w(x) \rightarrow \theta_s (\neq 0)$ as $x \rightarrow x_s$ in a singular way (Merkin [5]). In addition, for each case we have to check for singularity as well in determining the separation points x_s . For example, in the case of $Pr = 1$, the numerical solution indicates that the value of λ which first gives no separation lies between $\lambda = 0.34$ and $\lambda = 0.35$, and $x = \pi$ is the first boundary-layer separation point. At the point $x = \pi$, when we take $\lambda = 0.35$, the numerical solution indicates that there is no separation, but for $\lambda = 0.34$, we encounter singularity in the numerical solution. Hence, there exist no separation for values of $\lambda \geq 0.35$. Therefore, we conclude that the value of λ which first gives no separation lies between $\lambda = 0.34$ and $\lambda = 0.35$. However, the value of $\lambda = 0.35$ is determined and chosen after few trials. The other points of boundary-layer separation are determined in a similar way.

Representative results for the non-dimensional wall temperature distribution $\theta_w(x)$ and the skin friction coefficient C_f have been obtained at different positions x with various values of the mixed convection parameter λ when $Pr = 1$ and 7 , respectively.

In order to check the accuracy of the present method, the value of $g_0(0)$ for $Pr = 1$ has been calculated. Thus, we have obtained the value $g_0(0) = 1.9963$, which is in excellent agreement with those found by Merkin [13], $g_0(0) = 1.9963$, and by Yih [14], $g_0(0) = 1.9964$, respectively. Further, the values of $F''(0)$ and $\theta(0)$ obtained by numerically solving Eqs. (16) and (17) subject to the boundary conditions (18) for $Pr = 1$ and 7 , and some values of λ are

presented in Tables 1 and 2. The values obtained from the asymptotic series (31) for $\lambda (\gg 1)$ are also included in these tables and they show good agreement with the numerical values even at moderate values of λ . We are therefore confident that the results presented in this paper are very accurate.

Tables 3–6 show values of $\theta_w(x)$ and C_f at different positions x and different values of λ for $Pr = 1$ and 7 , respectively. The variation of $\theta_w(x)$ and C_f with x is also illustrated in Figs. 1–4. It can be seen from these tables and figures that the values of both $\theta_w(x)$ and C_f are lower for $Pr = 7$ than for $Pr = 1$ when the parameters x and λ are fixed. We can also conclude from these tables and figures that, as it is expected, the boundary-layer separates from cylinder for some negative values of λ (opposing flow) and also for some positive values of λ (assisting flow). Opposing flow brings the separation point close to the lower stagnation point and for sufficiently large negative values of λ or sufficiently strong opposing flow, there will not be a boundary-layer on the cylinder. Increasing λ delays the separation and that separation can be suppressed completely in the range $0 < x < \pi$ for sufficiently large values of $\lambda (> 0)$. Moreover, the numerical solutions indicate that the value of λ which first gives no separation lies between 0.34 and 0.35 for $Pr = 1$, while for $Pr = 7$ the value of $\lambda (> 0)$ lies between 1.49 and 1.50 , respectively.

The variation of the separation point x_s with λ is plotted in Figs. 5 and 6 for $Pr = 1$ and 7 , respectively. These figures show that for each value of Pr there is a value of $\lambda = \lambda_0 (< 0)$ below which a boundary-layer separation is not possible. The reason is that for $\lambda < 0$ the opposing flow is strong enough and the free convection boundary-layer would start at $x = \pi$ (the upper stagnation point), and for

Table 1. Values of $F''(0)$ and $\theta(0)$ for various values of λ and $Pr = 1$

λ	Numerical, Eqs. (16)–(18)		Series (31)	
	$F''(0)$	$\theta(0)$	$F''(0)$	$\theta(0)$
-1.2	-0.4394	2.1923		
-1.0	-0.1186	2.1687		
-0.8	0.1596	2.1545		
-0.6	0.4924	2.0547		
-0.4	0.7998	1.9046		
-0.2	1.0340	1.8157		
0.0	1.2336	1.7517		
0.2	1.4117	1.7018		
0.4	1.5747	1.6608		
0.6	1.7263	1.6260		
0.8	1.8690	1.5958		
1.0	2.0042	1.5692	1.9771	1.4447
1.4	2.2570	1.5239	2.2113	1.4294
1.8	2.4913	1.4863	2.4269	1.4050
2.2	2.7110	1.4542	2.6280	1.3800
2.6	2.9190	1.4262	2.8174	1.3560
3.0	3.1171	1.4015	3.0002	1.3340
4.0	3.5784	1.3500	3.4137	1.3057
5.0	4.0019	1.3088	3.8001	1.2500
6.0	4.3967	1.2746	4.1506	1.2202
7.0	4.7686	1.2455	4.4807	1.1888
8.0	5.1217	1.2201	4.8004	1.1612
9.0	5.4591	1.1977	5.1046	1.1404
10.0	5.7730	1.1770	5.4023	1.1200
20.0	8.5370	1.0482	7.9200	1.0035

Table 2. Values of $F''(0)$ and $\theta(0)$ for various values of λ and $Pr = 7$

λ	Numerical, Eqs. (16)–(18)		Series (31)	
	$F''(0)$	$\theta(0)$	$F''(0)$	$\theta(0)$
-2.5	-0.0251	1.1696		
-2.4	0.0101	1.1672		
-2.2	0.2436	1.0740		
-2.0	0.4159	1.0156		
-1.8	0.5401	0.9807		
-1.6	0.6459	0.9543		
-1.4	0.7391	0.9331		
-1.2	0.8238	0.9155		
-1.0	0.9015	0.9005		
-0.8	0.9748	0.8871		
-0.6	1.0441	0.8752		
-0.4	1.1100	0.8644		
-0.2	1.1730	0.8545		
0.0	1.2336	0.8455		
0.2	1.2919	0.8371		
0.4	1.3484	0.8293		
0.6	1.4030	0.8220		
0.8	1.4562	0.8152		
1.0	1.5079	0.8087	1.4953	0.6662
1.4	1.6075	0.7969	1.6010	0.7055
1.8	1.7028	0.7861	1.7014	0.7206
2.2	1.7943	0.7764	1.7967	0.7260
2.6	1.8824	0.7674	1.8875	0.7267
3.0	1.9676	0.7591	1.9744	0.7250
4.0	2.1697	0.7407	2.1773	0.7164
5.0	2.3590	0.7250	2.3640	0.7059
6.0	2.5379	0.7113	2.5382	0.6953
7.0	2.7081	0.6992	2.7024	0.6853
8.0	2.8710	0.6883	2.8583	0.6759
9.0	3.0275	0.6785	3.0072	0.6672
10.0	3.1785	0.6695	3.1501	0.6591
20.0	4.4811	0.6074	4.3634	0.6014

layer can exist at all on the cylinder for $\lambda < \lambda_0$ is still an open question.

Following Merkin [5], we can show that the separation of the boundary-layer will not occur for $\lambda > 1/\theta_w(x)$. To do it, we see from Eq. (13), that we get on $y = 0$

$$\left(\frac{\partial^3 \psi}{\partial y^3}\right)_{y=0} + (\lambda \theta_w(x) + \cos x) \sin x = 0 \tag{32}$$

Though $(\partial^2 \psi / \partial y^2)_{y=0} = 0$ at $x = x_s$, the streamwise velocity component $\partial \psi / \partial y$ will be positive near $y = 0$ and so $(\partial^3 \psi / \partial y^3)_{y=0} \geq 0$ at $x = x_s$. We thus have from Eq. (32) that $(\lambda \theta_w(x) + \cos x) \sin x \leq 0$, which cannot hold in the range $0 \leq x \leq \pi$ for $\lambda > 1/\theta_w(x)$.

Finally, Figs. 7–10 illustrate the velocity and temperature profiles near the lower stagnation point ($x \approx 0$) for $Pr = 1$ and 7, and for several values of λ . It is seen from these figures that, as it is expected, the temperature profiles increase and the velocity profiles decrease when the parameter λ decreases. However, these profiles are smaller for $Pr = 7$ than for $Pr = 1$. In addition, we notice that for $\lambda > 0$ (aiding flow) there is an overshoot of the velocity profiles from the free stream velocity, which is smaller for higher Prandtl number. However, the value of λ (> 0) for which this overshoot takes place is higher for $Pr = 7$ than for $Pr = 1$.

5 Conclusions

In this paper we have studied the problem of steady mixed convection boundary-layer flow over a horizontal circular cylinder with a constant surface heat flux, which is immersed in a viscous and incompressible fluid. We have sought to determine how the mixed convection parameter λ and the Prandtl number Pr affect the flow and heat transfer characteristics as well as the position of the boundary-layer separation point x_s . Solutions of the transformed non-similar boundary-layer equations are obtained numerically using the Keller-box method. From this study we can draw the following conclusions:

sufficiently small values of λ , there comes a point where the flow of the free stream upwards cannot overcome the tendency of the fluid next to the cylinder to move downwards under the action of the buoyancy forces (Merkin [5]). This is an unstable situation and whether a boundary-

Table 3. Values of the wall temperature distribution $\theta_w(x)$ for $Pr = 1$ and various values of λ

x	λ										
	-0.8	-0.6	-0.4	-0.2	0.0	0.2	0.34	0.35	0.5	1.0	5.0
0.0	2.1545	2.0547	1.9046	1.8157	1.7517	1.7018	1.6723	1.6704	1.6427	1.5692	1.3088
0.2	2.2201	2.0763	1.9169	1.8248	1.7593	1.7083	1.6783	1.6763	1.6482	1.5737	1.3112
0.4		2.1424	1.9513	1.8500	1.7799	1.7260	1.6946	1.6925	1.6632	1.5859	1.3177
0.6		2.3066	2.0135	1.8935	1.8147	1.7556	1.7216	1.7193	1.6879	1.6060	1.3282
0.8			2.1186	1.9597	1.8660	1.7984	1.7604	1.7579	1.7232	1.6343	1.3429
1.0			2.3257	2.0584	1.9376	1.8567	1.8125	1.8096	1.7701	1.6714	1.3619
1.2				2.2138	2.0369	1.9337	1.8802	1.8768	1.8303	1.7179	1.3852
1.4				2.5487	2.1783	2.0348	1.9668	1.9625	1.9058	1.7747	1.4131
1.6					2.4007	2.1692	2.0771	2.0715	1.9994	1.8427	1.4457
1.8					3.0241	2.3543	2.2183	2.2107	2.1147	1.9228	1.4836
2.0						2.6307	2.4019	2.3905	2.2561	2.0160	1.5272
2.2						3.1515	2.6456	2.6272	2.4285	2.1233	1.5775
2.4							2.9770	2.9443	2.6361	2.2456	1.6359
2.6							3.4284	3.3670	2.8801	2.3847	1.7053
2.8							4.0043	3.8906	3.1585	2.5455	1.7914
3.0								4.4986	3.4782	2.7441	1.9079
π								5.3220	3.7806	2.9456	2.0365

Table 4. Values of the local skin friction coefficient C_f for $Pr = 1$ and various values of λ

x	λ										
	-0.8	-0.6	-0.4	-0.2	0.0	0.2	0.34	0.35	0.5	1.0	5.0
0.0	0.0000	0.0000	0.0000	0.0000	0.0000	0.0000	0.0000	0.0000	0.0000	0.0000	0.0000
0.2	0.0170	0.0917	0.1547	0.2020	0.2421	0.2778	0.3009	0.3025	0.3259	0.3963	0.7947
0.4		0.1456	0.2816	0.3788	0.4600	0.5319	0.5783	0.5815	0.6282	0.7688	1.5595
0.6		0.1051	0.3550	0.5084	0.6331	0.7422	0.8121	0.8170	0.8871	1.0973	2.2683
0.8			0.3475	0.5721	0.7447	0.8926	0.9866	0.9931	1.0868	1.3656	2.8983
1.0			0.2097	0.5537	0.7827	0.9725	1.0912	1.0993	1.2168	1.5626	3.4311
1.2				0.4360	0.7410	0.9773	1.1218	1.1316	1.2729	1.6832	3.8535
1.4				0.1585	0.6175	0.9094	1.0811	1.0927	1.2578	1.7288	4.1575
1.6					0.4095	0.7774	0.9786	0.9920	1.1806	1.7064	4.3397
1.8					0.0408	0.5955	0.8296	0.8448	1.0560	1.6278	4.4002
2.0						0.3817	0.6544	0.6713	0.9028	1.5074	4.3411
2.2						0.1565	0.4765	0.4950	0.7414	1.3595	4.1643
2.4							0.3212	0.3404	0.5904	1.1959	3.8695
2.6							0.2107	0.2282	0.4617	1.0222	3.4503
2.8							0.1488	0.1614	0.3553	0.8347	2.8888
3.0								0.1078	0.2539	0.6147	2.1391
π								0.0303	0.1590	0.4068	1.4046

Table 5. Values of the wall temperature distribution $\theta_w(x)$ for $Pr = 7$ and various values of λ

x	λ										
	-2.0	-1.5	-1.0	-0.5	0.0	0.5	1.0	1.49	1.50	2.0	5.0
0.0	1.0156	0.9432	0.9005	0.8696	0.8450	0.8256	0.8087	0.7944	0.7941	0.7812	0.7250
0.2	1.0288	0.9506	0.9060	0.8742	0.8492	0.8291	0.8119	0.7973	0.7970	0.7839	0.7271
0.4		0.9716	0.9215	0.8868	0.8601	0.8386	0.8205	0.8052	0.8049	0.7912	0.7325
0.6		1.0114	0.9488	0.9085	0.8784	0.8546	0.8349	0.8184	0.8181	0.8034	0.7414
0.8			0.9926	0.9414	0.9054	0.8779	0.8557	0.8373	0.8369	0.8208	0.7540
1.0				0.9898	0.9433	0.9098	0.8836	0.8625	0.8621	0.8438	0.7704
1.2				1.0639	0.9961	0.9525	0.9202	0.8949	0.8945	0.8732	0.7908
1.4					1.0720	1.0095	0.9673	0.9359	0.9354	0.9097	0.8155
1.6					1.1927	1.0871	1.0279	0.9872	0.9865	0.9546	0.8448
1.8						1.1983	1.1064	1.0509	1.0499	1.0092	0.8791
2.0						1.3776	1.2097	1.1297	1.1284	1.0748	0.9188
2.2							1.3482	1.2268	1.2250	1.1529	0.9646
2.4							1.5343	1.3441	1.3416	1.2444	1.0176
2.6								1.4790	1.4756	1.3493	1.0801
2.8								1.6021	1.5988	1.4633	1.1572
3.0									1.6139	1.5654	1.2649
π									1.5620	1.6070	1.4095

Table 6. Values of the local skin friction coefficient C_f for $Pr = 7$ and various values of λ

x	λ										
	-2.0	-1.5	-1.0	-0.5	0.0	0.5	1.0	1.49	1.5	2.0	5.0
0.0	0.0000	0.0000	0.0000	0.0000	0.0000	0.0000	0.0000	0.0000	0.0000	0.0000	0.0000
0.2	0.0756	0.1332	0.1753	0.2108	0.2421	0.2707	0.2971	0.3214	0.3219	0.3453	0.4672
0.4		0.2367	0.3242	0.3966	0.4602	0.5178	0.5708	0.6195	0.6205	0.6674	0.9101
0.6		0.2813	0.4233	0.5362	0.6339	0.7213	0.8015	0.8747	0.8762	0.9464	1.3080
0.8			0.4502	0.6112	0.7464	0.8654	0.9734	1.0713	1.0732	1.1667	1.6438
1.0				0.6070	0.7862	0.9393	1.0761	1.1990	1.2014	1.3180	1.9056
1.2				0.5101	0.7471	0.9309	1.1060	1.2540	1.2569	1.3960	2.0869
1.4					0.6277	0.8664	1.0660	1.2392	1.2425	1.4032	2.1869
1.6					0.4266	0.7308	0.9660	1.1639	1.1677	1.3484	2.2100
1.8						0.5466	0.8218	1.0432	1.0474	1.2451	2.1645
2.0						0.3335	0.6548	0.8958	0.9003	1.1102	2.0604
2.2							0.4898	0.7419	0.7466	0.9608	1.9071
2.4							0.3538	0.5995	0.6040	0.8109	1.7109
2.6								0.4814	0.4853	0.6689	1.4720
2.8								0.4091	0.4113	0.5387	1.1802
3.0									0.4520	0.4322	0.8015
π									0.5421	0.3823	0.3979

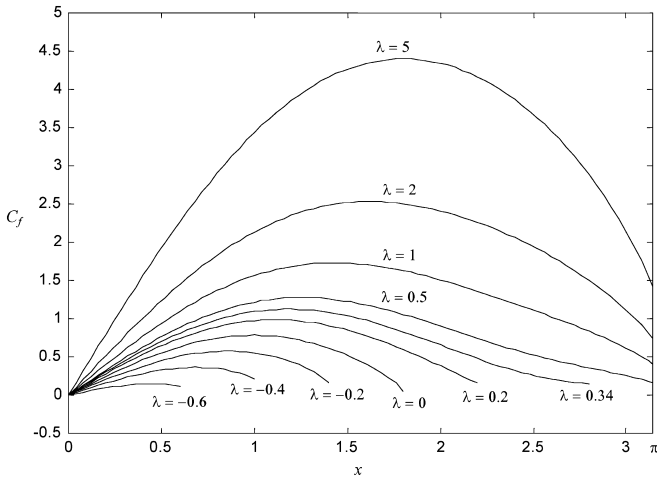


Fig. 1. Variation of the local skin friction coefficient C_f for $Pr = 1$ and various values of λ

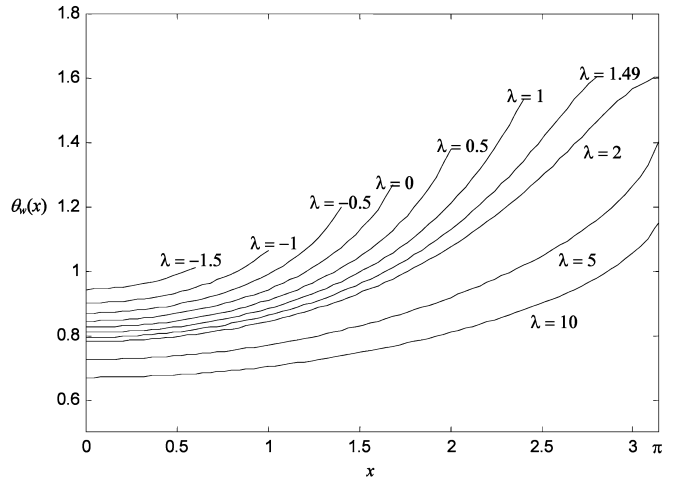


Fig. 4. Variation of the wall temperature distribution $\theta_w(x)$ for $Pr = 7$ and various values of λ

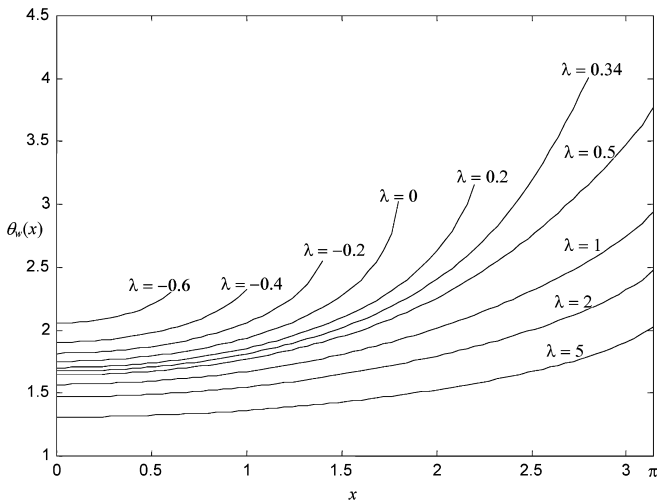


Fig. 2. Variation of the wall temperature distribution $\theta_w(x)$ for $Pr = 1$ and various values of λ

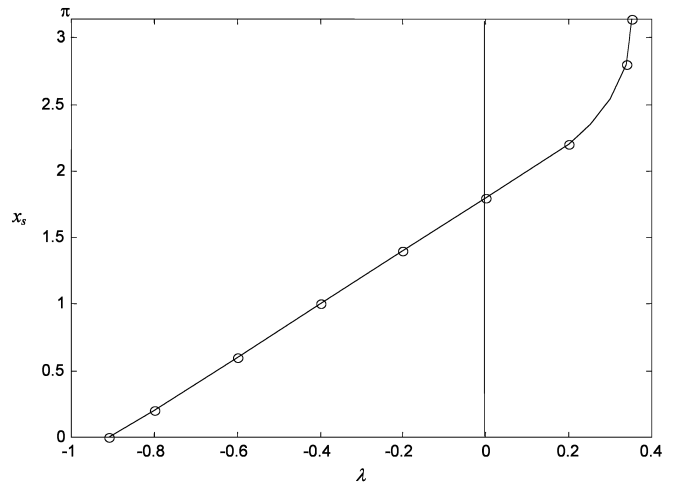


Fig. 5. Variation of the boundary-layer separation point x_s with λ for $Pr = 1$

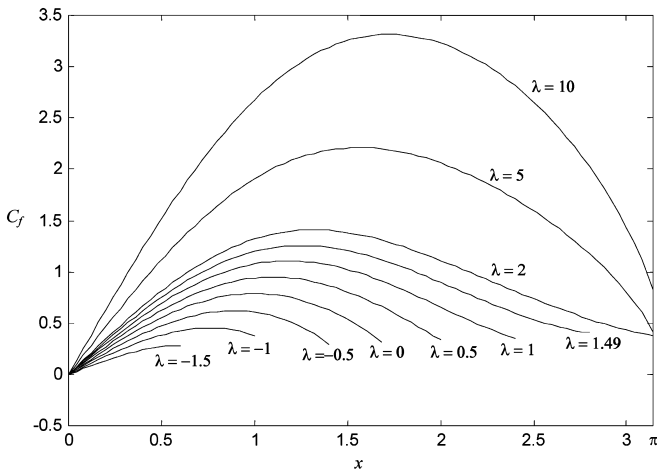


Fig. 3. Variation of the local skin friction coefficient C_f for $Pr = 7$ and various values of λ

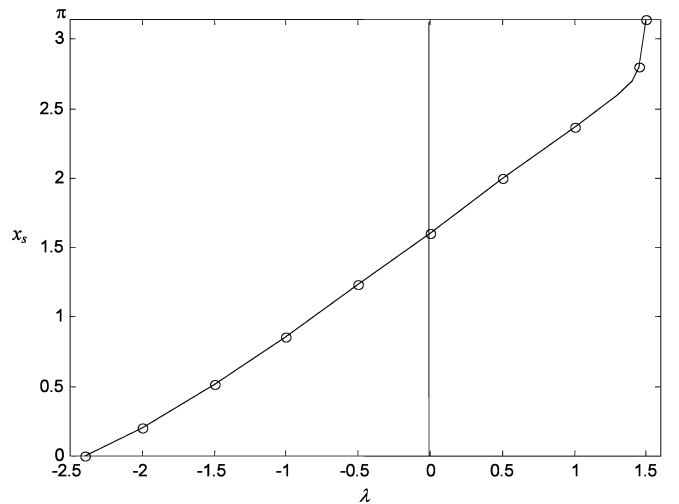


Fig. 6. Variation of the boundary-layer separation point x_s with λ for $Pr = 7$

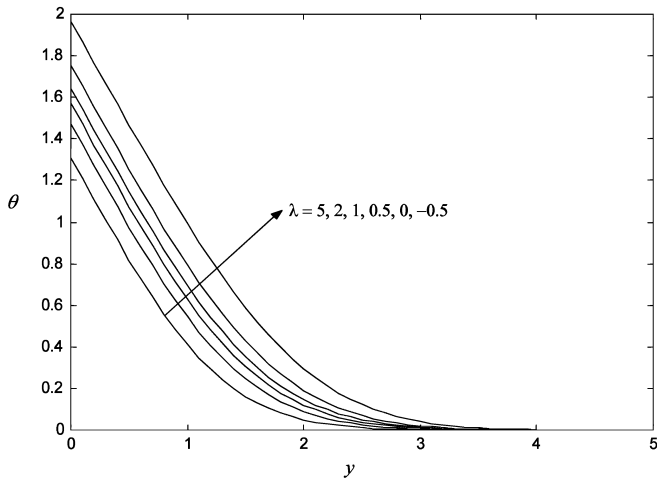


Fig. 7. Temperature profiles θ at $x = 0$ for various values of λ with $Pr = 1$

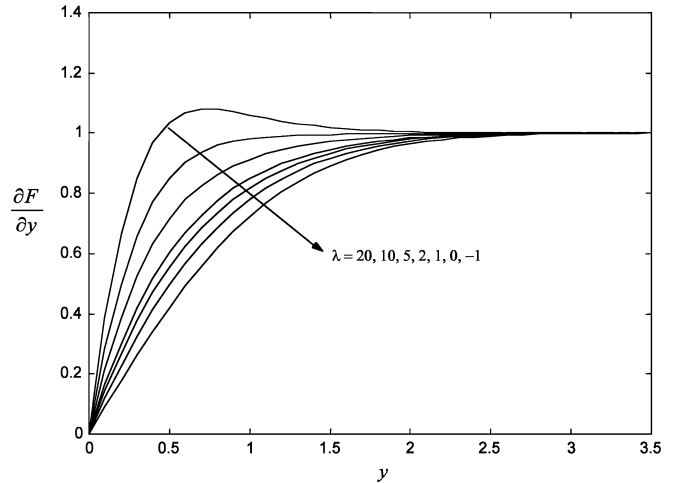


Fig. 10. Velocity profiles $\frac{\partial F}{\partial y}$ at $x = 0$ for various values of λ with $Pr = 7$

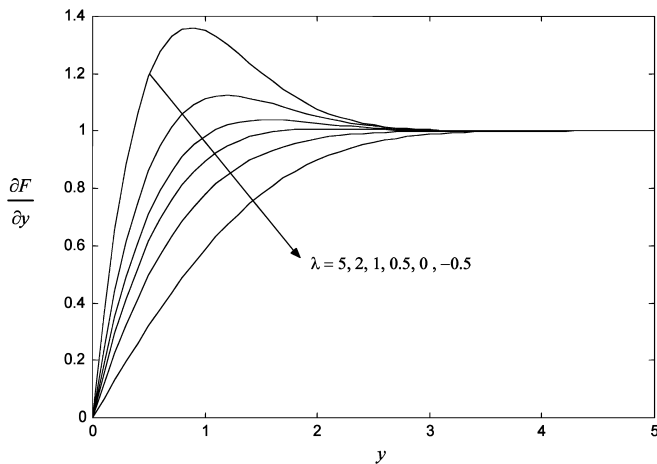


Fig. 8. Velocity profiles $\frac{\partial F}{\partial y}$ at $x = 0$ for various values of λ with $Pr = 1$

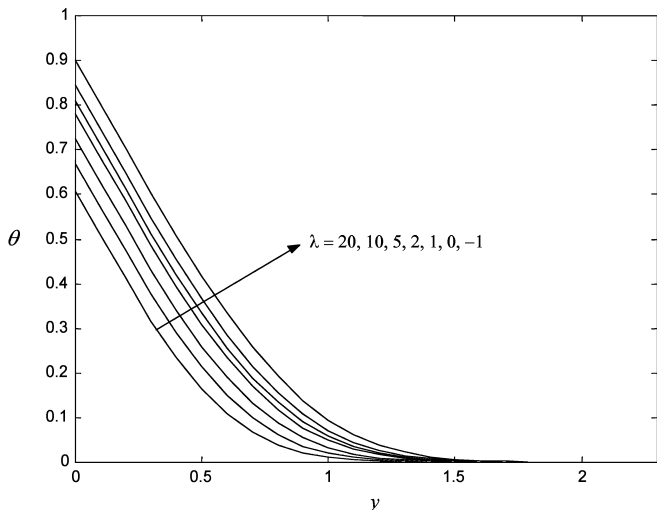


Fig. 9. Temperature profiles θ at $x = 0$ for various values of λ with $Pr = 7$

- an increase in the value of Pr leads to a decrease of both the wall temperature distribution $\theta_w(x)$ and the skin friction coefficient C_f
- an increase in the value of Pr leads to an increase of the value of λ (< 0) below which a boundary-layer solution is not possible
- an increase in the value of Pr leads to an increase of the value of λ (> 0) which first gives no separation
- near the lower stagnation point, the temperature profiles increase and the velocity profiles decrease when the parameter λ decreases
- there is an overshoot of the velocity profiles near the lower stagnation point from the free stream velocity

References

1. Acrivos A (1966) On the combined effect of forced and free convection heat transfer in laminar boundary layer flows. *Chem. Engng. Sci.* 21: 343–352
2. Joshi ND; Sukhatme SP (1971) An analysis of combined free and forced convection heat transfer from a horizontal circular cylinder to a transverse flow. *J. Heat Transfer* 93: 441–448
3. Nakai S; Okazaki T (1975) Heat transfer from a horizontal circular wire at small Reynolds and Grashof numbers – II. *Int. J. Heat Mass Transfer* 18: 397–413
4. Sparrow EM; Lee L (1976) Analysis of mixed convection about a horizontal cylinder. *Int. J. Heat Mass Transfer* 19: 229–232
5. Merkin JH (1977) Mixed convection from a horizontal circular cylinder. *Int. J. Heat Mass Transfer* 20: 73–77
6. Badr HM (1983) A theoretical study of laminar mixed convection from a horizontal cylinder in a cross stream. *Int. J. Heat Mass Transfer* 26: 639–653
7. Badr HM (1984) Laminar combined convection from a horizontal cylinder-parallel and contra flow regimes. *Int. J. Heat Mass Transfer* 27: 15–27
8. Aldoss TK; Ali YD; Al-Nimr MA (1996) MHD mixed convection from a horizontal circular cylinder. *Num. Heat Transfer, Part A.* 30: 379–396
9. Aldoss TK; Ali YD (1997) MHD free forced convection from a horizontal cylinder with suction and blowing. *Int. Comm. Heat Mass Transfer* 24: 683–693
10. Katagiri M; Pop I (1979) Unsteady combined convection from an isothermal circular cylinder. *J. Appl. Math. Mech. (ZAMM)* 59: 51–60

11. Ingham DB; Merkin JH (1981) Unsteady mixed convection from an isothermal circular cylinder. *Acta Mechanica* 38: 55-69
12. Cebeci T; Bradshaw P (1984) *Physical and Computational Aspects of Convective Heat Transfer*. Springer, New York
13. Merkin JH (1977) Free convection boundary layers on cylinders of elliptic cross section. *J. Heat Transfer* 99: 453-457
14. Yih KA (2000) Effect of uniform blowing/suction on MHD-natural convection over a horizontal cylinder: UWT or UHF. *Acta Mechanica* 144: 17-27